Magnetic Design of the Commutational Magnet and Quadrupoles for PERLE Accelerator

Journal of Physics: Conference Series **2687** (2024) 022023 doi:10.1088/1742-6596/2687/2/022023

Magnetic Design of the Commutational Magnet and Quadrupoles for PERLE Accelerator

R. Abukeshek[1], H. Abualrob[2], A. Stocchi[1], L. Perrot [1], A. Fomin [1], J. Michaud[1], A. Bogacz [3,*], J. Benesch [3,*], B. Jacquot [4]

[1] University Paris-Saclay, CNRS-IN2P3, IJCLab, Orsay, France
[2] An-Najah National University, Nablus, Palestine
[3] Jefferson Lab, CASA, Newport News, USA
[4] GANIL, Caen, France
[*] This work is supported by U.S. Department of Energy under DE-AC05-06OR23177

E-mail: rasha.abukeshek@ijclab.in2p3.fr

Abstract. PERLE (Powerful Energy Recovery LINAC for Experiment) is a three turns high-power Energy Recovery LINAC (ERL) facility with 20 mA beam current and beam energy from 250 MeV to 500 MeV. It is a testbed to validate multi-turn high current ERL operation for the future LHeC and will be the first ERL for nuclear applications. In this work, the design and optimization of the commutational magnet (B-com) used to spread/combine the three beams and one series of quadrupole magnets is discussed. The B-com magnet is optimized for a 30^o bending angle with harmonic content of 0.036%. The quadrupole magnets generate a field gradient of 34.15 T/m. Further studies to suppress saturation at a maximum gradient of 44.1 T/m are undergoing.

1. Introduction

Energy Recovery LINAC (ERL) [1] provides LINAC-like beam characteristics, and high average beam power in a more compact footprint than the storage ring. Up to date ERL facilities have been limited to ≤ 2 MW beam power in a single pass ERL [1]. Some new ongoing ERL facilities are Cornell-BNL Test Accelerator (CBETA) (USA) [2] and bERLinPro (Germany) [3]. PERLE [4] is three acceleration and three deceleration passes ERL accelerator with design parameters similar to those of the LHeC [5] (see Table 1).

PERLE is composed of three sections: the LINAC section at each straight line, the arc sections for beam recirculation, and the spreader/combiner section connecting the LINAC to the arcs. Figure 1 shows the 500 MeV first-order lattice of PERLE.

Vertical field dipoles and two families of quadrupole magnets are considered. The spreader/combiner sections accommodate commutational dipole (B-com magnet) [6] with horizontal magnetic field and a 30^o bending angle to split/combine the beam vertically at three different energies: 171 MeV, 336 MeV, and 500 MeV. A 8.842 cm vertical shift is required for the lowest energy beam. Normal conducting, Iron-dominated electromagnet technology is adopted to design PERLE magnets. Laminated steel ($< 0.1\%$ Carbon content) is used for the yoke.

The fundamental harmonic of the magnetic field produced by a pure vertical field dipole magnet is $B_y = C_1,\ B_x = 0$ and that produced by a quadrupole is $B_y = C_2 x,\ B_x = C_2 y$. In

Table 1: Input Design Parameters of PERLE Accelerator

Parameter	Value	Unit
Injection energy	7	MeV
Max. Beam energy	500	MeV
Beam rigidity	1.67	T·m
Injection beam current	20	mA
Bunch charge	500	pC
Bunch length	3	mm
Injection Bunch spacing	25	ns
Normalized emittance	6	mm·mrad
RF frequency	801.58	MHz
Duty factor	CW	

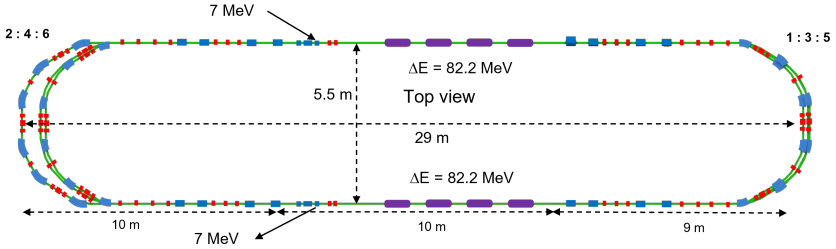

Figure 1: Footprint of 500 MeV PERLE accelerator with dipoles (blue) and quadrupoles (red).

practice, any fabricated magnet will produce a magnetic field with higher harmonics due to the finite geometry of the material called allowed harmonics. These are the $3, 5, 7, \ldots$ harmonics for dipole magnets and the $6, 10, 14, \ldots$ for quadrupole magnets. Non-allowed harmonics are present due to manufacturing tolerances. The symmetry of the yoke geometry can restrict the presence of higher-order harmonics. Higher-order harmonics degrade the field distribution and must be reduced for stable beam trajectory. Dipole field errors lead to undesired beam oscillation and quadrupole field errors lead to a tune shift [7].

The solution of Laplace's equation is used to calculate the pole shape. The excitation current NI required to drive the magnetic field in an electromagnetic dipole is $NI_{Dipole} = \frac{Bh}{2\mu_0}$ with N the number of coil turns, I the current, h the gap between the poles, μ_0 the magnetic permeability of free space. The excitation current in a quadrupole magnet is $NI_{Quadrupole} = \frac{Gr^2}{2\mu_0}$ with G the field gradient, r the magnet aperture. Dipole magnet pole shape follows $y = \pm\frac{h}{2}$. Quadrupole pole shape is a hyperbolic contour $xy = \pm\frac{r^2}{2}$ [7].

2. B-com Magnet Design

The design was carried out with Opera 3D, a finite element analysis software [8]. From the beam dynamics study of PERLE lattice, the beam size does not exceed 2 mm at 3σ (see Figure 2). Taking into account the thickness of the vacuum chamber, an aperture of 4 cm was chosen. The yoke is an H-shaped magnetic steel. The coil is made of a hollow Copper conductor based on water cooling. A blend radius of 0.8 cm was introduced to the pole edges to reduce the harmonic content. Figure 3 shows the B-com magnet design and Table 2 shows the main parameters of the coil.

Figure 3 shows a saturation in the pole edges. It can be suppressed by considering chamfer.

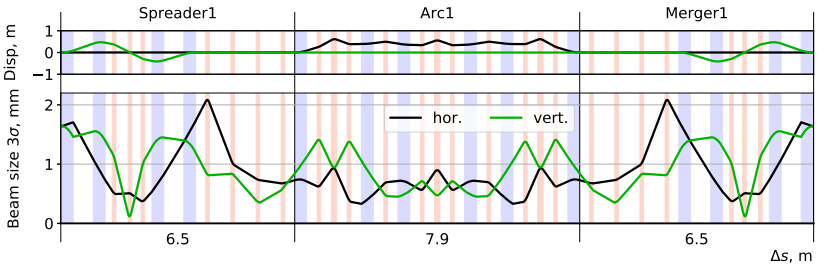

Figure 2: Electron beam envelope and dispersion function in the first arc section. Blue bars represent dipole magnets and red bars represent quadrupole magnets. The beam size is in mm corresponding to 3σ.

Table 2: Coil Design Parameters of PERLE B-com Magnet

Parameter	Value
Conductor width	8 mm
Conductor aperture	5 mm
Conductor corner radius	0.5 mm
Ampere-turns NI	11520.2625 A·turn
Number of turns/coil	30
Coil width	42.5 mm
Coil thickness	51 mm
Coil cross section	72.25 mm^2
Current	384 A
Current density	5.315 A/mm^2

Figure 4a shows the horizontal magnetic field component B_x along the pole width. It gives a field of 0.72 T at the center of the magnet. The field integral along the beam trajectory is 0.3 T.m. Figure 4b shows the field homogeneity (the variation of B_x along the pole width with respect to its value at the center B_0). B_x is homogeneous along ± 10 cm. Figure 5 shows that the lowest energetic beam exits the steel at 8.85 cm. The harmonic components of the magnet were calculated on a circle of 1 cm radius along the trajectory of the particles with 0.25 cm intervals. The square root of the sum of the harmonic coefficients squared is 0.036% on the lowest energy beam. The order of magnitude of the field homogeneity 10^{-4} meets the requirements for a successful beam separation/combination of 8.85 cm.

Figure 6 shows the value of the harmonic coefficients with respect to the fundamental harmonic b_1. The most dominant components are the quadrupole and sextupole ones which will be dealt with in the subsequent lattice elements of quadrupoles and sextupoles.

3. Quadrupole Magnet Design

Figure 7a shows the multi-coil design of the 15 cm length quadrupole magnet. The yoke is a cylindrical tube of 250 mm outer diameter with 35 mm thickness considering the 450 mm vertical separation between the arcs. Aperture radius of ± 20 mm is used to construct the hyperbolic pole profile of 44 mm width. Three hollow Copper conductor coils connected in series are considered to provide a less magnetic field in the pole base which is under 2 T (see Figure 7b). The current density in the three coils is 1.5 times less than that in a one-coil design of the same parameters. Table 3 shows the coil parameters.

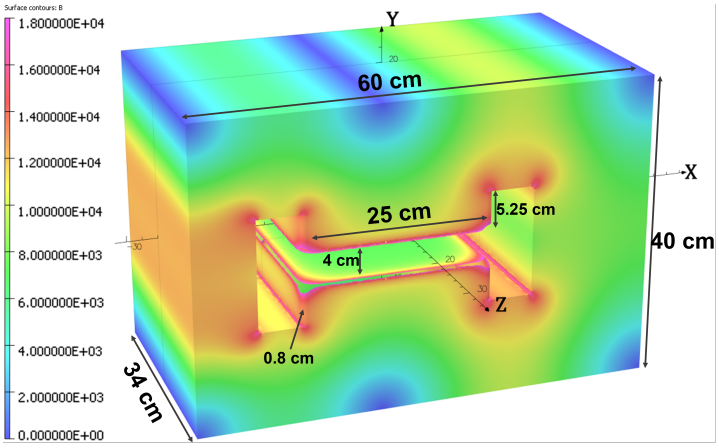

Figure 3: B-com magnet design with Opera 3D. The magnetic field is in Gauss. Areas with $B > 1.8\ T$ are not shown. Asymmetrical geometry was chosen for enhanced mechanical stability.

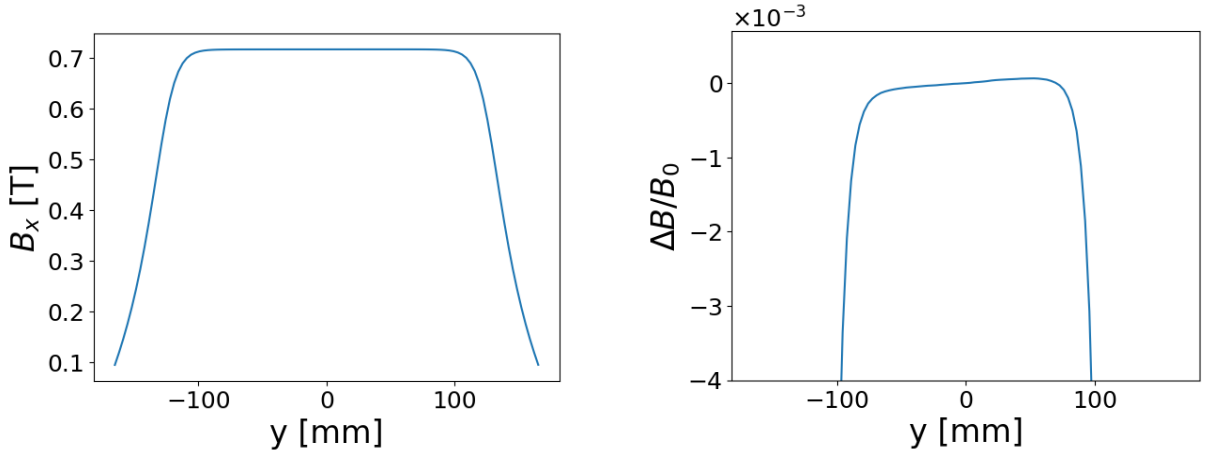

(a) (b)

Figure 4: (a) Vertical distribution of the horizontal magnetic field. (b) Field homogeneity along the pole width.

Table 3: Coil Design Parameters of PERLE Quadrupole Magnet

Parameter	Value
Conductor width	4 mm
Conductor aperture	2 mm
Conductor corner radius	0.5 mm
Excitation current	1750.7 A · turn
Number of turns/pole	20
Current	87.535 A
Coil cross-section	20.25 mm^2
Current density	2.882 A/mm^2

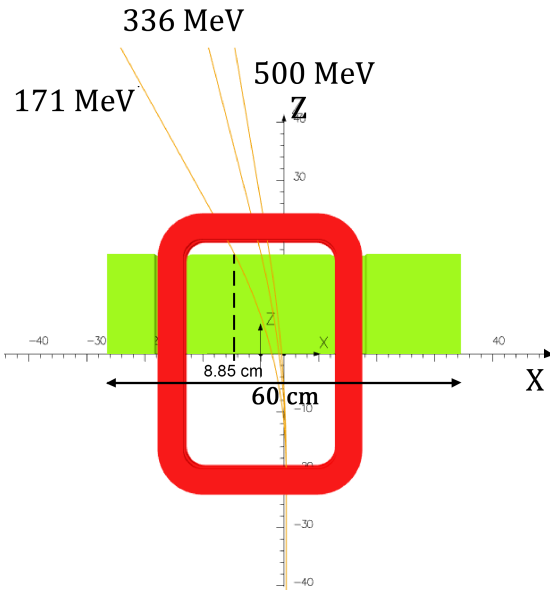

Figure 5: Trajectory of the electron beam through the B-com magnet at three energies: 171 MeV, 336 MeV, and 500 MeV. Initial position of the beam is (4.4,0,-60) cm.

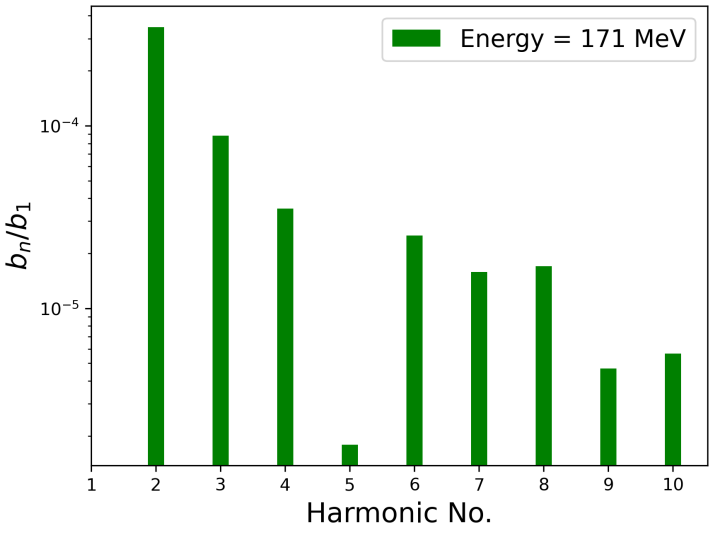

Figure 6: Higher harmonics with respect to the dipole component b_1 for electron energy of 171 MeV.

Figure 8 shows the vertical field component B_y as a function of the horizontal direction x. The gradient generated by the three-coil configuration is $G = 34.15$ T/m.

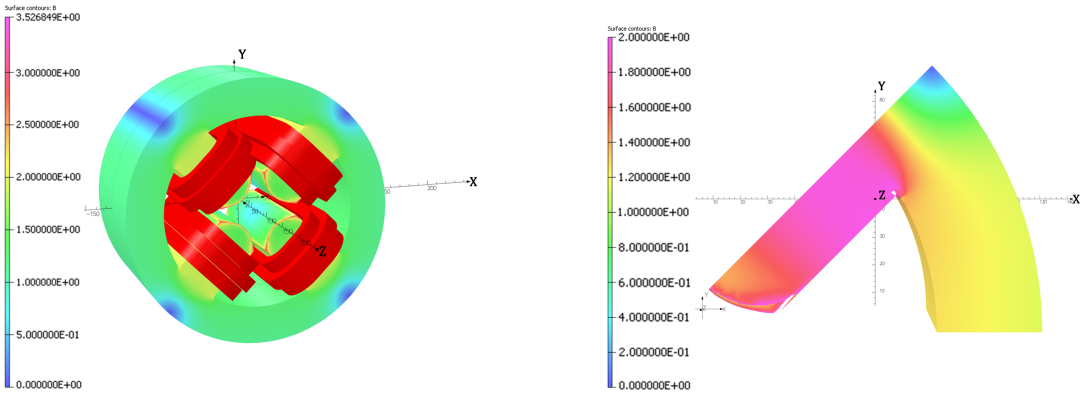

(a) (b)

Figure 7: (a) Three-coil quadrupole design of the l =15 cm quadrupole series of PERLE. (b) One octant of the quadrupole. Areas with a magnetic field higher than 2 T are not displayed.

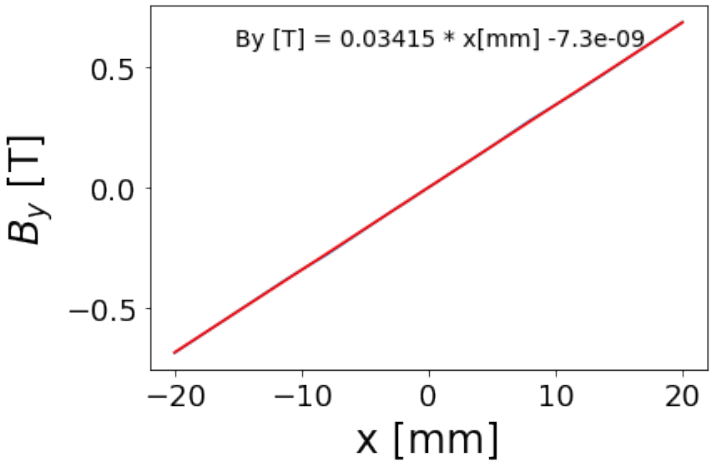

Figure 8: Horizontal distribution of the vertical magnetic field of the quadrupole.

4. CONCLUSION

The B-com magnet is optimized for a 30° bending angle with a harmonic content of 0.036%. The lowest energy beam exits the B-com magnet at a vertical distance of 8.85 cm. The quadrupole series of 15 cm length is designed to generate 34.15 T/m field gradient. Work is ongoing to increase this value to 44.1 T/m by introducing proper pole tapering. Beam dynamics study for the construction and optimization of the new PERLE machine of 250 MeV is ongoing and the updated parameters for the optics element will be considered to fully complete the design of the B-com magnet and start the fabrication process.

References

[1] C. Adolphsen, K. Andre, D. Angal-Kalinin, M. Arnold, K. Aulenbacher, S. Benson, J. Bernauer, A. Bogacz, M. Boonekamp and R. Brinkmann, *et al.*, "The Development of Energy-Recovery Linacs," *arXiv preprint*, 2022.
doi:10.48550/arXiv.2207.02095

[2] G. H. Hoffstaetter, D. Trbojevic, C. Mayes, N. Banerjee, J. Barley, I. Bazarov, A. Bartnik, J. S. Berg, S. Brooks and D. Burke, *et al.*, "CBETA Design Report, Cornell-BNL ERL Test Accelerator," *arXiv preprint*, 2017.
doi:10.48550/arXiv.1706.04245

[3] M. Abo-Bakr, W. Anders, Y. Bergmann, K. Bürkmann-Gehrlein, A. Bundels, A. Büchel, P. Echevarria, A. Frahm, H. W. Glock and F. Glöckner, *et al.*, "Status Report of the Berlin Energy Recovery Linac Project BERLinPro", in *Proc. IPAC'18*, Vancouver, Canada, Apr.-May 2018, pp. 4127–4130. doi:10.18429/JACoW-IPAC2018-THPMF034

[4] D. Angal-Kalinin, G. Arduini, B. Auchmann, J. Bernauer, A. Bogacz, F. Bordry, S. Bousson, C. Bracco, O. Brüning and R. Calaga, *et al.*, "PERLE. Powerful energy recovery linac for experiments. Conceptual design report," *J. Phys. G*, vol. 45, no. 6, p. 065003, 2018. doi:10.1088/1361-6471/aaa171

[5] J. L. Abelleira Fernandez *et al.* [LHeC Study Group], "A Large Hadron Electron Collider at CERN: Report on the Physics and Design Concepts for Machine and Detector," *J. Phys. G*, vol. 39, p. 075001, 2012. doi:10.1088/0954-3899/39/7/075001

[6] Leemann, Christoph W and Douglas, David R and Krafft, Geoffrey, "The continuous electron beam accelerator facility: CEBAF at the Jefferson Laboratory," *Annual Review of Nuclear and Particle Science*, vol. 51, no. 1, pp. 413–450, 2001. doi:10.1146/annurev.nucl.51.101701.132327

[7] D. Brandt, "Specialised course on Magnets", in *Proc. 2009 CAS-CERN Accelerator School*, Bruges, Belgium, June 16 - 25, 2009. doi:10.5170/CERN-2010-004

[8] 3DS SIMULIA DASSAULT Systems, Opera. https://www.3ds.com/products-services/simulia/products/opera/.